ISSN 2176-5480

22nd International Congress of Mechanical Engineering (COBEM 2013)
November 3-7, 2013, Ribeirão Preto, SP, Brazil

HIGH-SPEED IMAGING AND SPECTROSCOPIC MEASUREMENT OF THE BOUNDARY LAYER AROUND LANGMUIR PROBES IN HIGH-PRESSURE PLASMA

Louriel Oliveira Vilarinho
Federal University of Uberlandia, Laprosolda – Center for Research and Development of Welding Processes, Uberlandia, Brazil
vilarinho@mecanica.ufu.br

Laura Oliveira Vilarinho
CTBC/Algar Telecom; Uberlândia, MG, Brazil
laurav@algartelecom.com.br

Carlo Fanara
Cranfield University, UK

Abstract. *The extension of the plasma flow perturbation region forming around probes in TIG arcs has been measured for the first time. Emission spectroscopy readings were taken whilst probes were swept in arc using the two argon emission lines at 696.54 and 706.72 nm, whose intensities were compared with data taken in absence of probes. Several arc current values were investigated at few arc locations and it is shown that the thickness of the perturbed region is in broad agreement with numerical estimations performed elsewhere. Also, it decreases when the probe height in arc increases, and variations of its extension for different arc currents are discernible. Fast speed CCD camera photographs allow visualizing disturbances in the arc whilst swept by probes. These images show that the probe upstream region is less disturbed than the downstream region. As indications exist that charge capture prevails in the upstream region, the use of probes in this hostile environment can still be valuable. The photographs also suggest that increasing the arc length up to twice the usual 5 mm does not allow recovering the notion of free-stream and 'boundary layer' because of the up-scaling of the disturbance extension with increasing arc length.*

Keywords: *Welding, plasma, arc physics.*

1. INTRODUCTION

Atmospheric pressure arc plasmas, often referred to as “thermal plasmas” (Fauchais 1997) continue to offer challenges to the experimenter, especially technological ones like TIG arcs. Temperatures can be obtained from emission spectroscopy (Haddad 1984, Thornton 1993) although, due to the requirement of Local Thermodynamical Equilibrium (LTE), the technique is limited to the internal regions where the temperature exceeds about 10,000 K and/or to sufficiently high currents (greater than about 50 A). The alternative and cheaper Langmuir probe technique was attempted in (Gick 1973) and more recently in (Fanara 2001, Fanara 2003).

Although Langmuir probes have been extensively studied, a lack of results and further studies still remains for high-pressure arcs. Since the Langmuir probe is an invasive technique, it is very important to propose an experimental method to determine the extension of its disturbance. Also, the boundary layer estimation can be useful for the plasma temperature determination from plasma velocity (v_f) according to Ref. (Benilov 1989). A first relationship between the boundary layer thickness (δ) and v_f) is presented in Eq. (1) (Fanara 2003).

$$\delta = \frac{r_p}{\sqrt{R_e}} \tag{1}$$

where Re is the Reynolds number, given by $R_e = \dfrac{\rho\, v_f\, r_p}{\mu}$; r_p is the probe radius; ρ is the plasma density; and μ is the plasma dynamic viscosity.

By using Eq. 1, values between 45 and 220 μm were estimated for the boundary layer thickness (Fanara 2003). This result agrees with previous numerical results shown in Fig. 1. This figure confirms that increasing the current decreases the boundary layer thickness, which explains the practical experience in arc welding of stating that the lower the current, the more sensitivity arc is against external effects, such as environmental ones.

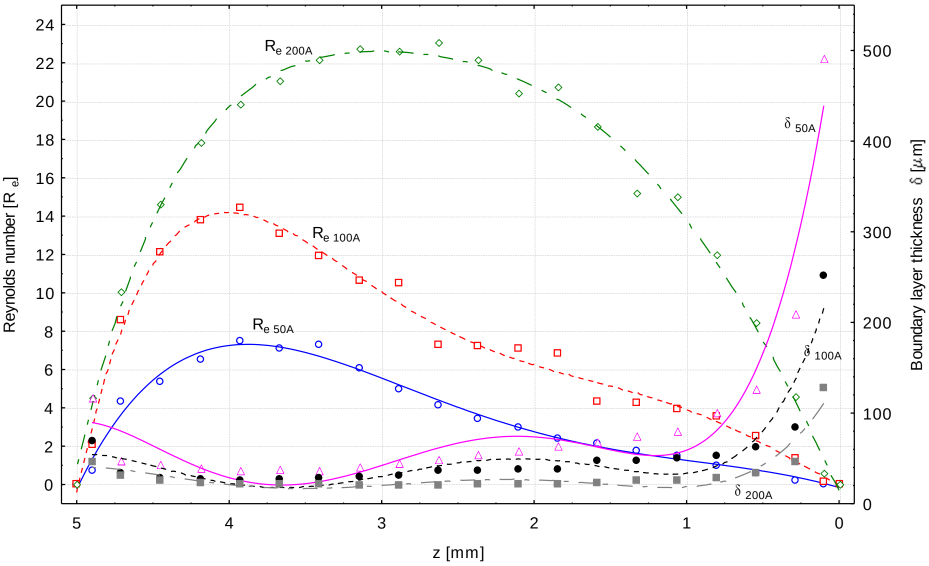

Figure. 1. Reynolds number and boundary layer thickness variation at the axis of an argon arc computed using previous (Vilarinho 2005) numerical results

Moreover, some numerical treatment for the plasma boundary layer estimation can be found in (Fay 1961, Fay 1963, Eckert and Pfender 1967, Cott 1971, Doss, Dwyer et al. 1974). Experimental estimation is presented by (Kimura and Kanzawa 1965, Bredfeldt, Scharfman et al. 1967), where two perpendicular Langmuir probes were employed and more recently by (Zhao, Owano et al. 2000), who studied boundary layers in C-H arcs at the anode with emission spectroscopy. Both numerical and experimental treatments are presented by (Suzuki and Kanzawa 1979).

A possibility for the boundary layer visualisation can be extracted from (Hauf and Grigull 1970). These authors presented a mathematical formulation considering the boundary layer acting as a schlieren lens. Therefore, once such perturbation region can be image, it is proposed to assess the possibility of the estimation of the boundary layer thickness in Langmuir probes by means of high-speed filming. Moreover, optical emission spectroscopy can be also employed as a comparison technique.

The importance of using emission spectroscopy remains on the fact that previous results (Fanara and Vilarinho 2004) have shown considerable differences between temperatures determined from the probe and the spectroscopic technique. It has been found that the interpretation of probe data in atmospheric pressure flowing arc plasmas is fraught with difficulties related to cooling effect which originate from the arc flow (Benilov 1989, Fanara 2003, Fang 2003). A complete arc characterization including temperature determination is possible if the flow velocity and the extension of the probe perturbed region are available. In this case, theories incorporating flow (Benilov 1989, Benilov 1991) could enable the experimenter to correct the probes characteristic curves in the ion saturation region in order to obtain the number density (Benilov 1991, Fanara 2002) or the temperature under various hypotheses about the probe current (Gick 1973, Fanara 2003). Indications exist (Fang 2003) that the gradients of the flow velocity within the probe perturbed region are very high and the analytical or modelling problem becomes very difficult if not impossible.

Therefore, the aim of this paper is to evaluate the typical extension of the boundary layer forming around probes when sweeping in atmospheric pressure arcs by using both emission spectroscopy and high-speed filming.

2. EXPERIMENTAL APPROACH

2.1 Setup

The experimental setup was developed for dedicated probe and spectroscopic measurements (Fanara, 2001 and 2003). The set-up for arc striking and probe rotation is presented in Fig. 2. Probes, made of copper with 58 mm length and 250 μm diameter, are swept through the arc at a velocity of 5 m/s for their entire length in order to avoid end-point effects. A high-speed camera (model Phantom® V4.0) with digital image output was employed with a 500-mm focal lens in order to provide 6x zoom. The camera was set at 2000 fps with a resolution of 512x256 pixels and 0.5 s of analysis interval. An exposure time of 10 μs per frame (shutter) was used in order to avoid blur images. The camera was placed at 2380 mm from the arc centre on a 16° angle. This was done because the spectrometer was in a perpendicular view, so the camera must be place aside of it. The need of the 16° angle implies in a correction on the dimensions taken from images of 1.08, i.e., sqrt(1+sin216)/cos16 (Vilarinho, 2002).

For the spectroscopic measurements, the light from the arc is directed to the entrance slit of a 1 m Czerney-Turner monochromator (Jobin-Yvon 1704, 1200 grooves/mm, reciprocal linear dispersion of 0.8 nm/mm for first order images)

ISSN 2176-5480

equipped with a CCD detector. Light from the arc is imaged at a 1:1 ratio on to a 50-µm diameter pinhole. Light from the pinhole is collected by a second lens and imaged to the monochromator entrance slit (50 µm width, 3 mm height). Two argon spectral lines (Ar I 696.54 and 706.72 nm) intensities from different locations in the arc are recorded as a function of position in absence and in presence of probes.

A DC arc is struck between a tungsten electrode (cathode) and a copper anode. The cathode is a 3.2-mm diameter, 2% thoriated (AWS EWTh-2), typically ground to a 60º include angle and truncated to a 0.2-mm flat tip. The anode is a 36-mm diameter and 6-mm thick oxygen free copper disk hosted in a copper block and can be readily substituted for each run. The anode block is cooled in order to prevent melting and to avoid evaporation which would alter the thermal and physical properties of the arc (metal vapour impurities have a lower ionisation potential). A series regulated power supply is used (model GEC AWP H350sr), to provide a highly uniform output (current ripples less than ± 0.1 A).

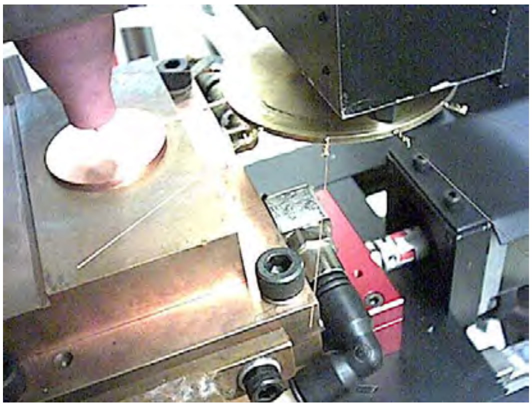

Figure 2. Experimental rig for probe measurements

The probe oscillation, resultant of motor shaft allowances, is a critical factor in this system. Different attempts were made in order to reduce the motor shaft oscillation, which should run true (“perfectly” aligned). However, some oscillation was verified. The probe oscillation was measured by using a telescopic vernier as 140 µm.

2.2 Methodology

The principle of the method is to scan the chosen arc locations using two argon emission lines (previously employed to determine the temperature in the work of Fanara, 2002 and Vilarinho, 2002) in absence and in presence of probes and compare the absolute intensities (in this paper emphasis is given to ArI 696.54-nm line) Because the timing for the optical and the probe experiments is quite different, in order for the method to work a sufficient number of probes is inserted at the same height within the arc. This allows appreciating the variation of the intensity with the arc height. The first attempt to determine the boundary layer extension was employing two probes as shown in Fig. 3. The reason for employing a smaller number of probes was the difficulty of aligning different probes at the same height. The next attempt was made with ten probes. The results (Fig. 3) clearly show the existence of the boundary layer. It must be pointed out that the continuum intensity did not show any variation due to the probe insertion into the plasma. This very first result presents a thicker boundary layer than it was expected (maximum of 500 µm according to Fig. 1). Besides the measured probe oscillation (140 µm), the intrinsic probe fluctuation when it passes through the arc could lead to further increase in the boundary layer measurement.

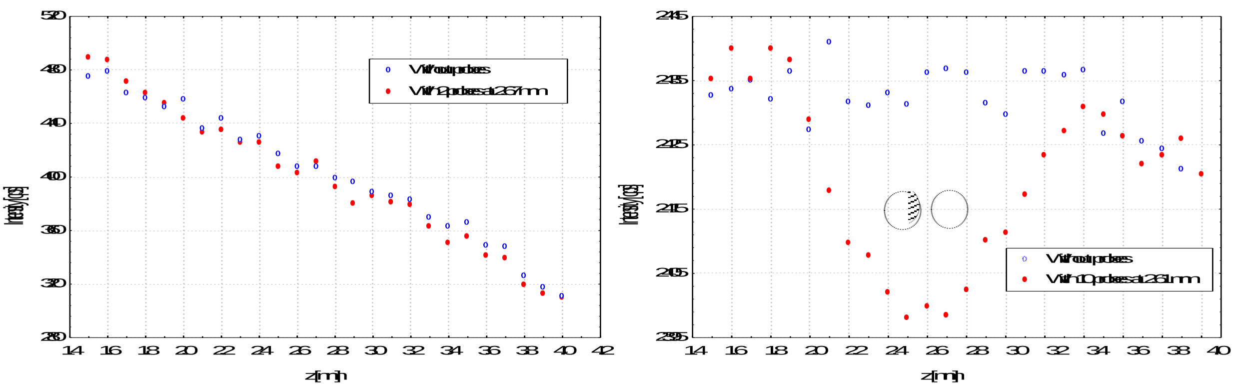

Figure 3. Line intensities with height position for ArI 696.54 nm when two (left) and ten probes (right) are in a 50-A arc

ISSN 2176-5480

From this result, ten probes were placed at the same position and the arc spectrum in the range of 696.54 and 706.72 nm were acquired. Three different measuring positions in the arc were investigated: at 1.25-mm; 2.5-mm height and 3.75-mm height, all at radius equal zero. For each of these five positions, a vertical distance of 1.25 mm around them was covered with a step of 100 μm, totalling 26 points. Each of these 26 points is made of five sampling in order to provide a good average. Initially, a comparison between ten and five sampling was made and the differences between the two means were less than 5 %.

An important feature of the experimental rig for high-speed filming is the diaphragm aperture or f-number. The f-number is the ratio between the focal distance of the objective lens and the real aperture of the diaphragm. For instance, since in this case a 500-mm lens was employed, if an aperture of f22 is selected, the diaphragm diameter would be 22.7 mm. On the other hand, if f4 is used the diaphragm would have a diameter of 125 mm. This observation results that the lower the aperture the more light will reach the camera CMOS. Thus, it was investigated the influence of the aperture in the range of f22, f16, f11, f8, f5.6 and f4, i.e., diaphragm diameters of 22.7, 31.25, 45.45, 62.5, 89.29 and 125 mm.

Since it is difficult for a human eye to observe contrasts in arc images, the images obtained here will be processed and their colour maps will be changed from RGB-24bits to HSV (hue-saturation-value colour map). An HSV colour map varies the hue component of the hue-saturation-value colour model. The colours begin with red, pass through yellow, green, cyan, blue, magenta, and return to red. There are also other colour maps that can be used, for instance grey, hot, cool, bone, copper, pink, flag, prism, jet. Among them, the HSV standard seemed more appropriated in this case, due to the high contrast obtained (Vilarinho 2002).

An experimental confirmation of the arc disturbance by the probe can be obtained using a high-speed camera for filming the probe while passing through the arc. Some examples of the original high-speed images can be seen in the sequences presented in Fig. 5. From this figure, it is possible to assert that, although it is difficult to precisely determine the boundary layer, the Langmuir probes disturb the arc. One can see the bottom of the arc shrinking when the probe is inside the arc, p. ex. the 3rd frame of Fig. 5.

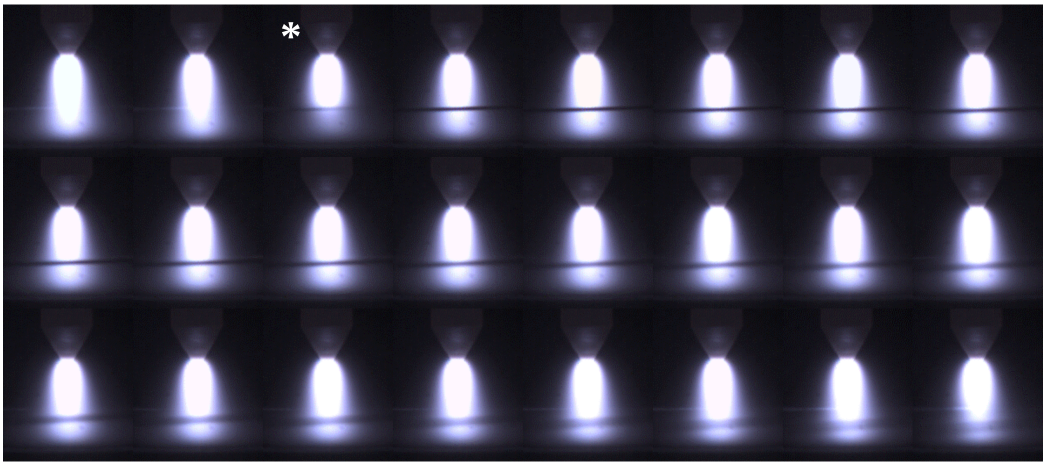

Figure 5. High-speed images for 70-A argon arc, f8 and probes at 2.5 mm (frame interval equal to 0.5 ms). The asterisk indicates the frame in which the probe crosses the arc

3. RESULTS AND DISCUSSION

Basing on the aperture investigation and the final quality of the HSV images, the following values were selected for analyses in the range 200 A to 50 A in pure Ar arc with 5 mm of length, because their lowest saturation condition: 200A – f22; 150 A – f22; 100 A – f22; 70 A – f16 and 50 A – f11. For 10-mm arcs, the following values were used: 200A – f22; 100 A – f16 and 50 A – f8. The current levels of 150 A and 70 A were not used for 10-mm arc because the objective is to show a trend of comparison between the two arc lengths (5 and 10 mm).

The final images are shown in Figs. 6 and 7 respectively for 5-mm and 10-mm arcs and for the three positions of the probes (1.25-mm; 2.5-mm and 3.75-mm height). These images clearly show the arc disturbance and a perturbation region (PR) located after the arc passes the probe, i.e., a downstream PR exists when probes are inserted in TIG arcs.

From these images the colour profile in the centre of each image was extracted and it was plotted against the height as shown in Fig. 8 and 9, for 5-mm and 10-mm arcs, respectively. For the 5-mm arcs spectroscopic measurements were also taken as comparison with the images and plotted in Fig. 8 for each probe position at the same time high-speed filming were done. Note that in all the curves showing the emission intensity as a function of height, the flow is oriented from high to low z (e.g. right to left, cathode to anode). In all cases, a well is visible, whose extension, corresponding to the approximate PR (Perturbation Region) thickness, is obtained from the intercepts of the two curves (the pictorial full circles, approximately to scale, represent the probe section).

ISSN 2176-5480

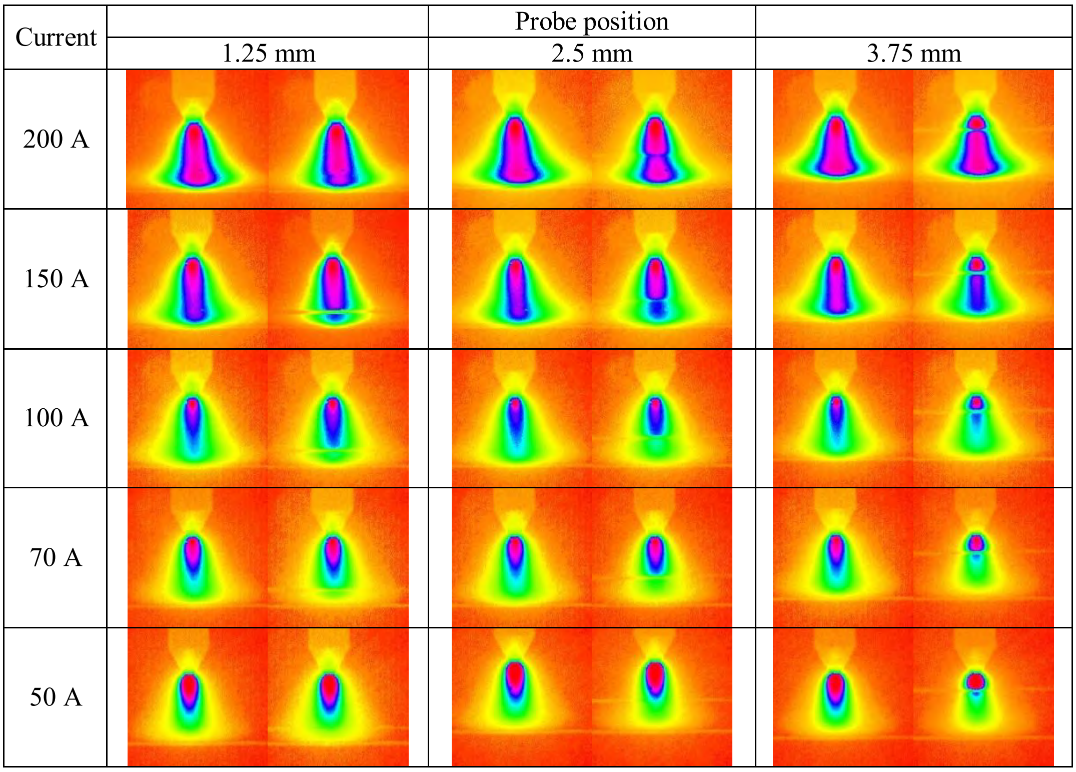

Figure 6. Arc length 5 mm left image (no probe), right image (with probe)

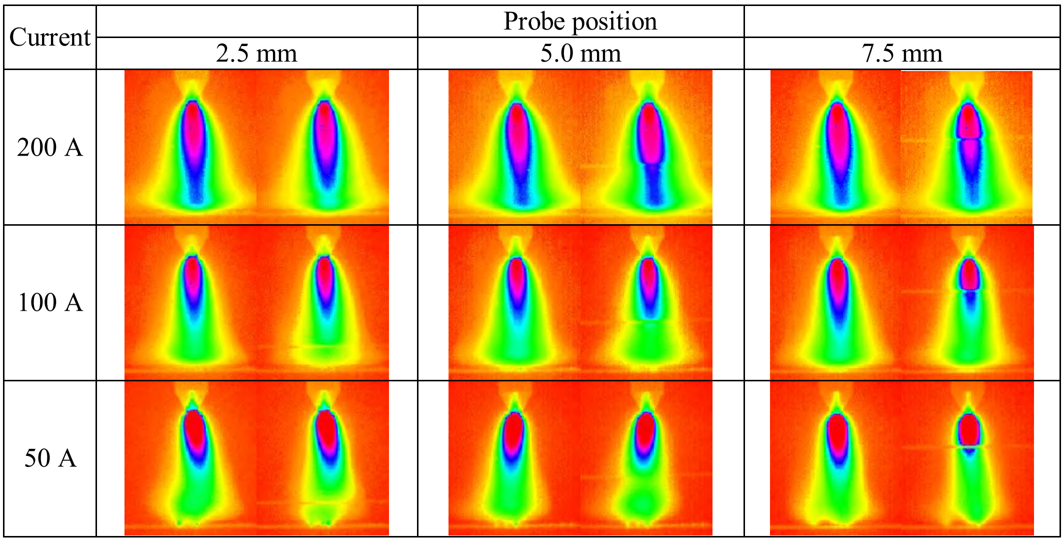

Figure 7. Arc length 10 mm left image (no probe), right image (with probe)

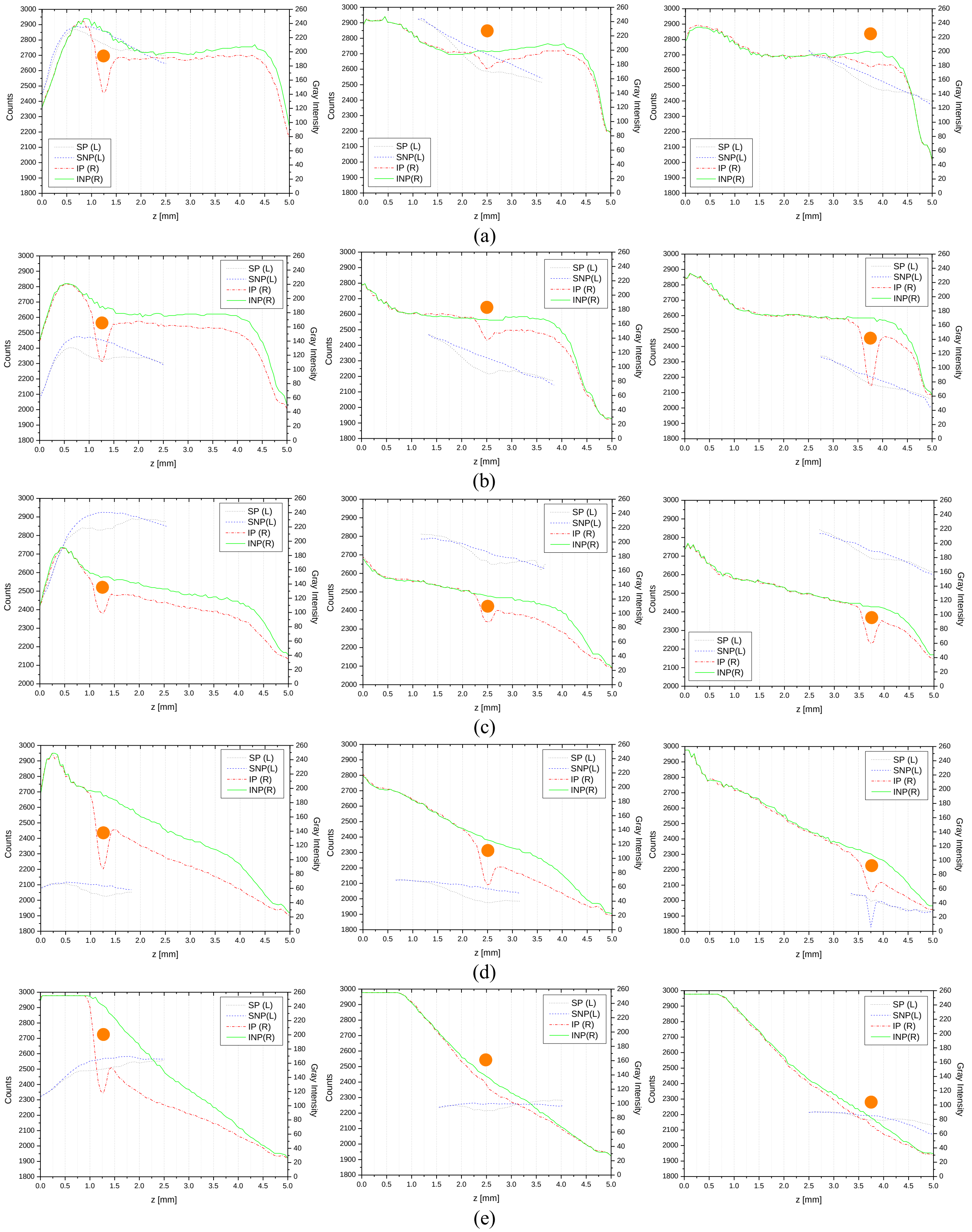

Figure 8. Comparison between spectroscopic and high-speed filming measurement for 5-mm arcs at (a) 200 A, (b) 150 A, (c) 100 A, (d) 70 A and (e) 50 A with probe height position at 1.25 mm (left images); 2.5 mm (center images) and 3.75 mm (right images): SP – Spectroscopy with probe, SNP – Spectroscopy without probe, IP – Image with probe, INP – Image without probe, (L) – Left axis, (R) – Right axis and Probe diameter (orange circle) = 250 µm

ISSN 2176-5480

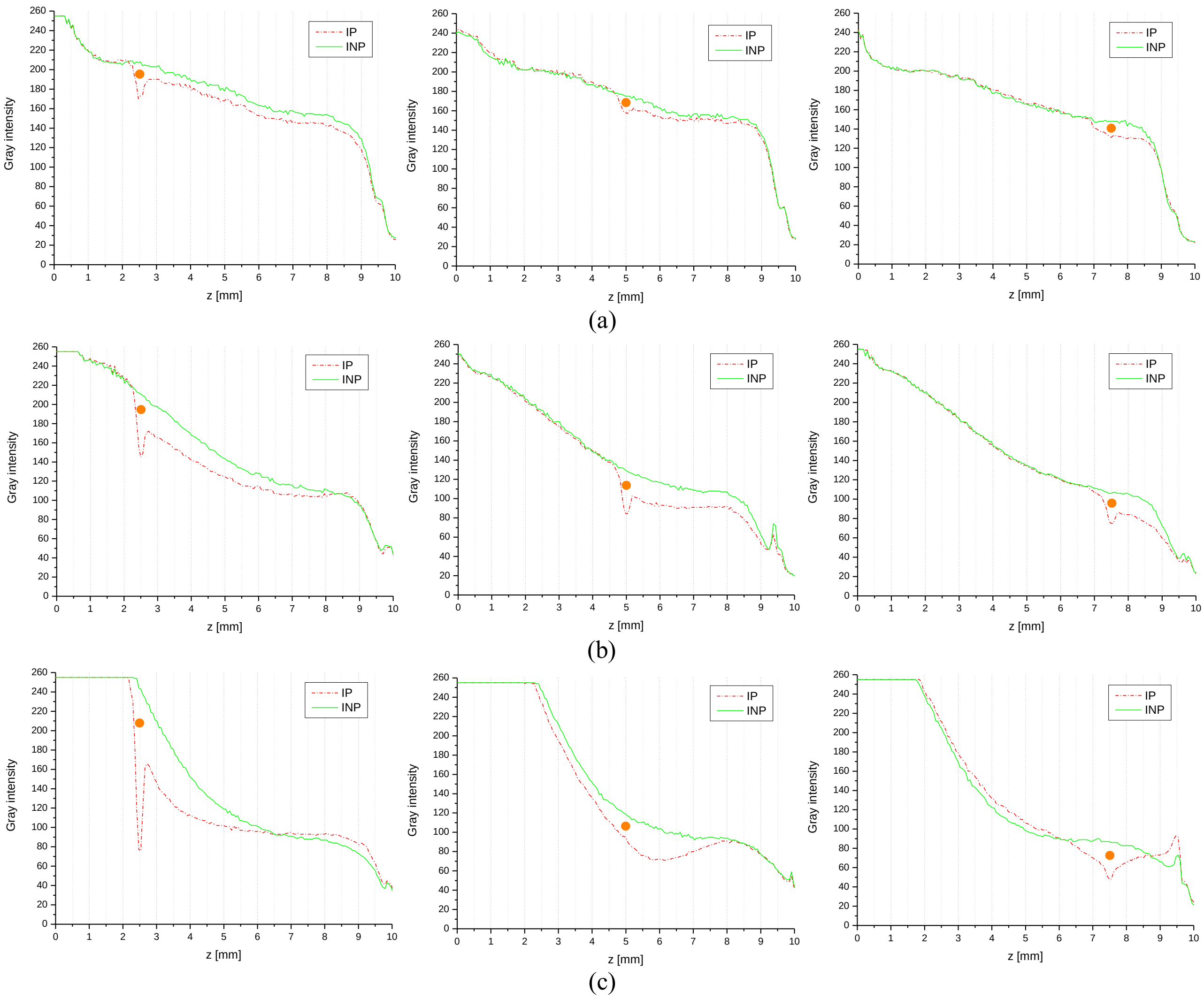

Figure 9. High-speed filming measurement for 10-mm arcs at (a) 200 A, (b) 100 A and (c) 50 A with probe height position at 1.25 mm (left images); 2.5 mm (center images) and 3.75 mm (right images): IP – Image with probe, INP – Image without probe and Probe diameter (orange circle) = 250 µm

The variation of the integrated intensity with the arc height, non-monotonic, is consistent with the expected behaviour of the emission coefficient as a function of height. In fact, the arc cross section decreases as the arc height increases, causing a lowering of the integrated intensity. In contrast, the intensity increases as the temperature rises with the arc height. These two effects can be appreciated observing the number of counts for the 'blanks' between the different axial regions, which, as they should, match in the complete curves, 0 to 5 mm.

The comparison between the curves obtained with and without probes as a function of the height z gives an appreciation of the PR extension. The difference of the intensity counts is lower at higher probe position. This suggests that the probe shielding (e.g. the masking of the light by the probes) is less marked at higher axial positions. As noted earlier, the greater the height, the smaller the arc section. Thus the (line) integrated intensity is lower for both signals and blanks. If this reduction, due to the smaller section, is the same with and without probes, the reduced contribution of the signals with probe would dominate. However, this assumption implies undisturbed arc, thus to avoid circular argument, a series of photographs was taken to check for discernible variations of the arc diameter at the probe chosen height. Thus the line integrated intensity is reduced by the combined effect of probe shadowing under 'undisturbed conditions' and by the arc radius reduction.

From Figs 8 and 9, it can be observed that the width of the perturbation region is always lower as the arc height increases, with the exception of the case I=50 A. Also, there are indications that at mid-arc the up- and downstream portions of the PR are the same. This is expected because in the region closer to the cathode the flow velocity is higher and in the idealized free-stream conditions one would expect a thinner boundary layer.

Of central importance is the interpretation to attribute to the measured thickness. Should the conditions allow for the existence of a free-stream, the PR could be identified with the boundary layer and an estimate could be attempted of the velocity at the edge? However, the extension of this PR is of an order of magnitude comparable with the overall

ISSN 2176-5480

length of the plasma arc in the 5 mm point-plane geometry. The latter circumstance makes the mentioned identification unjustified.

In fact, the complete sequence of photographs at different currents of the arc core, where velocity and temperature gradients are steeper, and of the envelopes, indicates that the perturbation takes place beyond the expected 'Boundary layer' extension allowed by a free-stream theory, estimated previously in a fraction of a millimetre, as discussed in Fig. 1. However, because in Fang (2003) it is concluded that, in identical conditions, the probe disturbance in a 5 mm arc extends for the whole arc length, and that ‘there are no localized un-disturbed upstream conditions’, photographs were taken at a longer arc length (L=10 mm for Fig. 9) to verify the presence of up-scaling of the PR thickness with the arc length and, possibly, to visualize the up- and down-stream differences shown by the spectroscopic measurements. It should be noted that comparison between arcs with same current but different lengths must be performed with some caution. Augmenting the arc length under the same conditions decreases the power density and therefore the light emission (for instance, the picture of a 200 A arc at L=10 mm is similar to the appearance of a 5 mm arc at 50 A).

With this limitation in mind, a visual inspection of Fig. 8 for the 200-A 5-mm case and Fig. 9 for the 200-A 10-mm case suggests comparable fractional up scaling of the PR extensions: the overall PR amounts in both cases to 30 to 35% of the arc length; the upstream extension is 1 to 2% of the arc length and the remaining of the PR is due to the downstream portion of the PR. The asymmetry tends to disappear for lower probe positions (below mid-arc, towards the anode). This is in qualitative agreement with the spectroscopic measurements. Therefore, despite the semi-quantitative nature of the photographic analysis, two conclusions are possible: (1) there is clear asymmetry between the up- and down- stream probe regions at high arc length and (2) the PR extension increases with the arc length. In the first instance, there is some experimental evidence (Tsuij, 1973) of orientation dependent charge capture on cylindrical probes, with 'active' surface variable from half to two-thirds of the upstream probe surface (Tsuij, 1973 and Benilov 1991). A similar statement, concerning the majority of the charge collection taking place at the upstream side of a probe in a flowing plasma, although unreferenced, is reported in Clements (1977). If this is correct, the fact that the PR is less extended upstream of the probe indicates that the relevant plasma parameters could be obtained from the upstream surface within the limitation of a ‘small’ disturbance. Therefore, for this purpose, the found asymmetry between up- and downstream regions could be ignored in probe data analysis. However, the second conclusion indicates that a distance of 10 mm is still too short to recover free-stream conditions. One possible outcome of these results is that the upstream condition could be an indicative of the anode region in TIG arcs.

4. CONCLUSIONS

It has been shown that emission spectroscopy and high-speed filming can be used to estimate the extension of the perturbation region (PR) arising around Langmuir probes in atmospheric pressure flowing plasmas. The extension of the PR can be quantified in a few probe diameters and shows the very perturbative nature of the probe method in short arc plasmas (5 to 10 mm) at all the currents examined. The monotonic decrease of the PR depth with increasing distance from the anode has also been obtained. Asymmetry in the probe up- and down-stream regions was shown both by spectroscopic measurements and high-speed filming.

5. ACKNOWLEDGEMENTS

The authors would like to thank to Fapemig (under Proc. TEC-PPM-00511-12), to CNPq (under Procs. 481975/2012-8 and 307710/2011), to Laprosolda/UFU, to CTBC/Algar Telecom and to CAPES/PROEX.

6. REFERENCES

Benilov, M. S. 1989. "Theory of electrical probes in flows of high-pressue weakly ionized plasma." *High Temperature* 26(5): 780-793.

Benilov, M. S. 1991. "Ion saturation currents to spherical and cylindrical electrostatic probes in collisional plasmas." *Journal of Applied Physics*, 70(11): 6726-6731.

Bredfeldt, H. R., W. E. Scharfman, H. Guthart and T. Morita 1967. "Boundary-layer Ion Density Profiles as Measured by Electrostatic Probes." *AIAA Journal* 5(1): 91-98.

Clements, R. M., Oliver, B.M., Smy, P.R. 1977. "Pulsed spherical probe measurements of plasma conductivity in a flowing continuum plasma." *Journal of Physics D: Applied Physics* 10: 2213.

Cott, D. W. 1971. "Ionizational and Electron Thermal Nonequilibrium in MHD Boundary Layers." *AIAA Journal* 9(12): 2404-2410.

Doss, E. D., H. A. Dwyer and M. A. Hoffman 1974. "Influence of Segmentation and Ambipolar Diffusion on MHD Nonequilibrium Boundary Layers." *AIAA Journal* 12(2): 155-162.

Eckert, E. R. G. and E. Pfender 1967. *Advances in Plasma Heat Transfer. Advances in Heat Transfer*. J. P. Hartnett and T. F. I. Jr., Academic Press. 4: 228-316.

Fanara, C. 2003. “A multi-langmuir probe for the characterization of atmospheric pressure plasmas”, *PhD thesis*, Cranfield University.

Fanara, C., Richardson, I.M. 2001. "A Langmuir multi-probe system for the characterization of atmospheric pressure plasmas." *Journal of Physics D: Applied Physics* 34: 2715-2725.

Fanara, C. and Vilarinho, L. O. 2004. "Electrical Characterization of Atmospheric Pressure Arc Plasmas - an Overview." *European Physical Journal D* 28: 241-251.

Fanara, C., Vilarinho, L.O. 2002. “Optical and electrical measurements in atmospheric pressure arcs: a comparison”. *Annual Gaseous Electronics Conference* (GEC02), Minneapolis, MN, USA, October 15-18 2002.

Fang, M. T. C., Zhang, JinLing, Yan, J.D. 2003. “Can Langmuir Probe be used for the diagnostics of atmospheric thermal plasmas with gas motion?” Paper ISPC-343. *16th International Symposium on Plasma Chemistry*, Taormina (Italy), 22-27 June 2003.

Fauchais, P., Vardelle A. 1997. "Thermal plasmas." *IEEE Transactions on Plasma Science* 25(6): 1258.

Fay, J. A. 1961. *Plasma Boundary Layers*. Cambridge, MA, MIT: 18.

Fay, J. A. 1963. *Energy Transfer in a Dense Plasma*. Cambridge, MA, MIT: 16.

Gick, A. E. F., Quigley, M.B.C., Richards, P.H. 1973. "The use of electrostatic probes to measure the temperature profiles of welding arcs." *Journal of Physics D: Applied Physics* 6: 1941.

Haddad, G. N., Farmer, A.J.D. 1984. "Temperature determinations in free burning arc: I. Experimental techniques and results in argon." *Journal of Physics D: Applied Physics* 17: 1189-1196.

Hauf, W. and Grigull, U. 1970. “Optical Methods in Heat Transfer”. *Advances in Heat Transfer*. J. P. Hartnett and T. F. I. Jr., Academic Press. 6: 133-366.

Kimura, I. and Kanzawa, A. 1965. "Experiments on Heat Transfer to Wires in a Partially Ionized Argon Plasma." *AIAA Journal* 3(3): 476-481.

Suzuki, M. and Kanzawa, A. 1979. "Boundary-layer Charged-Particle Density Profiles in an Atmospheric Pressure Plasma Flow." AIAA Journal 17(12): 1320-1325.

Thornton, M. F. 1993. Spectroscopic determination of temperature distributions for a TIG arc, *Ph.D. Thesis*, Cranfield University.

Tsuij, H., Toshisuke, H. 1973. "Ion current distribution around an electrically conductive body in ionized gas flow." *AIAA J.* 11(1): 100-102.

Vilarinho, L. O. 2001. Assessment of shielding gases by means of numerical and experimental techniques, *Qualification Exam*, UFU, Brazil, 201 p.

Vilarinho, L. O. 2002. Optical emission spectroscopy. Cranfield, *Internal Report Cranfield University*.

Vilarinho, L. O. 2005. "Welding Arc Modelling: a Survey." *Soldagem e Inspecao* 10(1): 38-46.

Zhang, J. 2004. "Private Communication."

Zhao, M., T. G. Owano and Kruger, C. H.. 2000. *Boundary Layer Diagnostics of an Atmospheric Pressure Plasma Jet*: 7p.

7. RESPONSIBILITY NOTICE

The authors are the only responsible for the printed material included in this paper.